Membrane Transport, Structure, Function, and Biogenesis:

The Ubiquitin Isopeptidase UBPY Regulates Endosomal Ubiquitin Dynamics and Is Essential for Receptor Down-regulation

Paula E. Row, Ian A. Prior, John McCullough, Michael J. Clague and Sylvie Urbé

J. Biol. Chem. 2006, 281:12618-12624.
doi: 10.1074/jbc.M512615200 originally published online March 6, 2006

THE JOURNAL OF BIOLOGICAL CHEMISTRY VOL. 281, NO. 18, pp. 12618–12624, May 5, 2006

The Ubiquitin Isopeptidase UBPY Regulates Endosomal Ubiquitin Dynamics and Is Essential for Receptor Down-regulation*

Received for publication, November 28, 2005, and in revised form, February 22, 2006 Published, JBC Papers in Press, March 6, 2006, DOI 10.1074/jbc.M512615200

Paula E. Row, Ian A. Prior[1], John McCullough, Michael J. Clague, and Sylvie Urbé[2]

From the Physiological Laboratory, University of Liverpool, Crown Street, L69 3BX Liverpool, United Kingdom

UBPY is a ubiquitin-specific protease that can deubiquitinate monoubiquitinated receptor tyrosine kinases, as well as process Lys-48- and Lys-63-linked polyubiquitin to lower denomination forms *in vitro*. Catalytically inactive UBPY localizes to endosomes, which accumulate ubiquitinated proteins. We have explored the sequelae of short interfering RNA-mediated knockdown of UBPY. Global levels of ubiquitinated protein increase and ubiquitin accumulates on endosomes, although free ubiquitin levels are unchanged. UBPY-depleted cells have more and larger multivesicular endosomal structures that are frequently associated through extended contact areas, characterized by regularly spaced, electron-dense, bridging profiles. Degradation of acutely stimulated receptor tyrosine kinases, epidermal growth factor receptor and Met, is strongly inhibited in UBPY knockdown cells suggesting that UBPY function is essential for growth factor receptor down-regulation. In contrast, stability of the UBPY binding partner STAM is dramatically compromised in UBPY knockdown cells. The cellular functions of UBPY are complex but clearly distinct from those of the Lys-63-ubiquitin-specific protease, AMSH, with which it shares a binding site on the SH3 domain of STAM.

Activated receptor tyrosine kinases (RTK)[3] generally enter the endosomal system through incorporation into clathrin-coated vesicles and delivery to a tubulo-vesicular compartment known as the early or sorting endosome. From here receptors may recycle to the plasma membrane or be selected for lysosomal sorting by incorporation into small vesicles that bud away from the limiting membrane into the vacuolar lumen to generate multivesicular bodies (MVBs) (1–3). Activated RTKs such as epidermal growth factor (EGF) receptor (EGFR), platelet-derived growth factor receptor, and Met are multimonoubiquitinated through the action of an E3 ubiquitin ligase, the proto-oncogene c-Cbl (4–7). Ubiquitination provides a sorting signal that is proposed to engage with the MVB sorting machinery through an initial interaction with the UIM (ubiquitin interacting motif) domain of Hrs (hepatocyte growth factor receptor tyrosine kinase substrate) (8–10).

Classical studies elucidated polyubiquitin chains linked through an internal lysine (Lys-48) as a proteasomal degradation signal (11–13). However, there is an increasing appreciation that alternative polyubiquitin chain structures play crucial roles in cellular physiology (14, 15) and that ubiquitination is a dynamic post-translational modification, which may come to rival phosphorylation in its scope and complexity. The reversibility of ubiquitination can be attributed to the action of deubiquitinating enzymes (DUBs) of which there are an estimated 79 encoded in the human genome (16, 17).

Two DUBs, associated molecule with the SH3-domain of STAM (AMSH) and ubiquitin-specific processing protease Y (UBPY) are known to interact directly with signal transducing adapter molecule (STAM), a protein that is constitutively associated with the endosomal sorting adapter Hrs (18, 19). In fact, they share a binding site on the SH3 domain of STAM by virtue of a conserved binding motif, P*X*V/ID/NR*XX*KP (19). AMSH is a member of the JAMM/MPN+ family of metalloproteases (20, 21), which we have shown to negatively regulate EGFR sorting to the lysosome as evidenced by enhanced receptor degradation following acute stimulation of AMSH knockdown cells (22). UBPY is a cysteine protease of the ubiquitin-specific processing protease (UBP/USP) family, also known as USP8, and has been proposed to regulate cellular ubiquitin levels and entry into S phase (23). The yeast orthologue of UBPY is thought to be Doa4, which associates with late components of the MVB sorting machinery (24, 25) and has been proposed to recycle ubiquitin from committed receptors (26, 27). In this paper we show that knockdown of UBPY by RNA interference has multiple cellular effects that include the accumulation of ubiquitinated proteins on endosomes, an increase in both number and size of multivesicular endosomes, and a block in RTK degradation.

EXPERIMENTAL PROCEDURES

Plasmids—Human UBPY cDNA was obtained from the Kazusa DNA Research Institute, Japan (clone KIAA0055) and subcloned into pEGFP-C1. The C786S mutation was introduced by QuikChange site-directed mutagenesis (Stratagene) and subcloned into pEGFP-UBPY. A short interfering (si)RNA-resistant UBPY construct (UBPY*) was generated by introducing five degenerate point mutations (underlined below) into UBPY within the region targeted by UBPY-specific siRNA duplex1 (forward primer sequence GCCTATGTACTATATATGAAGTAC-GTCACGGTGTACAATCTTATC) and subcloning into pEGFPC1-UBPY. GST-UBPY, HA-STAM, and Flag-ubiquitin constructs were generous gifts from Giulio Draetta (Milan, Italy), Naomi Kitamura (Yokohama, pMIW-HA-Hbp), and John O'Bryan (Chicago, IL).

Antibodies and Other Reagents—Mouse monoclonal anti-HA antibody was from Covance, and anti-ubiquitin antibodies were from Sigma (U5379), Covance (P4G7), and Affiniti-Biomol (FK1, FK2). Anti-GFP was a gift of Francis Barr (Martinsried, Germany). Mouse monoclonal anti-EGFR R1 and goat polyclonal anti-EGFR 1005 were from Santa Cruz. Met antibodies were obtained from Cell Signaling. Anti-lysobisphosphatidic acid was a generous gift of Jean Gruenberg (Geneva, Switzerland). Rabbit polyclonal AMSH, Hrs, and STAM antibodies

* This work was supported by a Wellcome Trust Career Development Award (to S. U.). The costs of publication of this article were defrayed in part by the payment of page charges. This article must therefore be hereby marked "*advertisement*" in accordance with 18 U.S.C. Section 1734 solely to indicate this fact.

[1] A Royal Society University Fellow.

[2] To whom correspondence should be addressed. Tel.: 44-151-794-5432; Fax: 44-151-794-4434; E-mail: urbe@liv.ac.uk.

[3] The abbreviations used are: RTK, receptor tyrosine kinase; MVB, multivesicular bodies; EGF, epidermal growth factor; EGFR, EGF receptor; DUB, deubiquitinating enzyme; UBPY, ubiquitin-specific processing protease Y; STAM, signal transducing adapter molecule; siRNA, short interfering RNA; HA, hemagglutinin; GFP, green fluorescent protein; BES, 2-[bis(2-hydroxyethyl)amino]ethanesulfonic acid; SH, Src homology; E3, ubiquitin-protein isopeptide ligase.

have been previously described (7, 22, 28, 29) Secondary antibodies were from Molecular Probes and Sigma. Protein A- and G-agarose were from Sigma.

Bacterial Expression and Purification of Recombinant Proteins—GST-UBPY was expressed in Rosetta (DE3) pLysS cells (Novagen) and batch-purified with glutathione-Sepharose (Pharmacia) according to manufacturers' instructions. Purified protein was dialyzed against DUB-assay buffer.

Deubiquitination Assays—Lys-48-linked tetraubiquitin (250 ng) or Lys-63-linked tetraubiquitin chains (250 ng) (Boston Biochem) were incubated for 2 h at 37 °C in 20 μl of DUB-assay buffer (50 mM Tris/HCl, 25 mM KCl, 5 mM $MgCl_2$, 1 mM dithiothreitol), pH 8.3, with 1 μM GST-UBPY. Proteins were resolved on 4–12% NuPAGE gels (Invitrogen) according to manufacturer's instructions. Resolved proteins were transferred to nitrocellulose (0.2 μm), the membrane was boiled for 30 min in deionized water, blocked in 0.5% fish skin gelatin, 0.1% Tween 20 in phosphate-buffered saline, and probed with a rabbit antibody to ubiquitin (Sigma) followed by ECL-based detection.

Cell Culture and Transfection—HeLa cells were cultured in 5% CO_2 in Dulbecco's modified Eagle's medium supplemented with 10% fetal calf serum and 1% non-essential amino acids. All tissue culture reagents were purchased from Invitrogen. HeLa cells were transfected with GeneJuice transfection reagent (Merck Biosciences) and lysed or fixed 24 h post-transfection.

Cell Lysis and Immunoprecipitation—Cells were washed twice in ice-cold phosphate-buffered saline and lysed in Nonidet P-40 lysis buffer (0.5% Nonidet P-40, 25 mM Tris/Cl, pH 7.5, 100 mM NaCl, 50 mM NaF). Lysates were cleared by centrifugation and incubated with antibodies and Protein A- or Protein G-agarose for 2 h at 4 °C. Alternatively, cells were lysed in "hot SDS" lysis buffer (1% SDS, 50 mM NaF, 1 mM EDTA at 110 °C), and lysates were heated at 110 °C for 10 min with intermittent vortexing, precleared by centrifugation at 14,000 rpm for 5 min, and diluted with four volumes of TX100-dilution buffer (1.25% TX100, 25 mM Tris, pH 7.5, 125 mM NaCl, 50 mM NaF) prior to immunoprecipitation.

Detection of Ubiquitinated EGFR—siRNA-treated cells were starved in serum-free medium for 16 h, stimulated with 100 ng/ml EGF for various times, placed on ice, and lysed in radioimmune precipitation assay buffer (10 mM Tris/HCl, pH 7.5, 100 mM NaCl, 1% (w/v) Nonidet P-40, 0.1% (w/v) SDS, 1% (w/v) sodium deoxycholate, and 50 mM NaF), supplemented with protease inhibitors, phosphatase inhibitors, and 10 mM *N*-ethylmaleimide. EGFR was immunoprecipitated overnight and immunoprecipitates were washed in 20 mM Tris/HCl, 150 mM NaCl, and 0.1% Nonidet P-40 and resuspended in sample buffer. Three-quarters of each sample was analyzed by immunoblotting with anti-ubiquitin, and the remainder was probed in parallel for EGFR, to control for even loading.

Depletion of Cellular UBPY by siRNA—HeLa cells were treated twice over 96 h with either control siRNA duplex (nonspecific control VII) or UBPY-specific siRNA duplex1 (sense UGAAAUACGUGACUGUUUAUU, antisense 5′-PUAAACAGUCACGUAUUUCAUU) or UBPY-specific siRNA duplex 2 (sense GGACAGGACAGUAUAGAUAUU, antisense 5′-PUAUCUAUACUGUCCUGUCCUU, Dharmacon, Lafayette, CO) and AMSH-specific siRNA duplex (sense UUACAAAUCUGCUGUCAUUUU, antisense 5′-PAAUGACAGCAGAUUUGUAAUU, Dharmacon) at 40.8 nM concentration using Oligofectamine in the absence of serum (Invitrogen). Four hours post-transfection, fetal bovine serum was added to a final concentration of 10%. Alternatively, HeLa cells were treated twice over 96 h with siRNA at a concentration of 47.2 nM using a calcium phosphate protocol. Briefly, medium was replaced with 10 ml of Dulbecco's modified Eagle's medium + 10% fetal bovine serum, 500 μl of 0.25 M $CaCl_2$, and 0.52 nmol of siRNA were premixed and added gradually with gentle vortexing to 500 μl of BBS (50 mM BES, pH 6.95, 280 mM NaCl, 1.5 mM Na_2HP0_4), incubated for 20 min and added dropwise to the cells. The cells were then incubated at 3% CO_2 overnight. The efficiency of UBPY knockdown was routinely assessed by Western blotting and determined manually by counting on a fluorescence microscope the percent of cells showing an accumulation of ubiquitin on endosomes as shown in Fig. 5*E*. For the siRNA-rescue experiment, HeLa cells were treated twice over 96 h with either control siRNA duplex or UBPY-specific siRNA duplex1. Sixty-six hours before harvesting, the cells were transfected with pEGFPC1 or pEGFPC1-siRNAi resistant UBPY (UBPY*). The percent of GFP-labeled cells, which retained EGFR after 4 h of EGF treatment was determined manually by counting on a fluorescence microscope.

Immunofluorescence—Cells were processed 24 h post-transfection for immunofluorescence as previously described (8). Secondary antibodies used were labeled with Alexa-Fluor 594 or 488. Dual-stained confocal images were taken with a Leica confocal SP2 AOBS (HCX PL APO CS 63.0 × 1.40 oil objective).

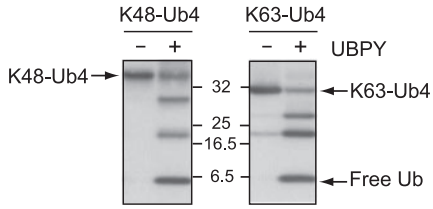

FIGURE 1. **UBPY converts both Lys-48 and Lys-63-linked ubiquitin chains.** GST-UBPY (1 μM) was incubated with enzymatically produced wild-type Lys-48- or Lys-63-linked tetraubiquitin chains (250 ng, 0.34 μM) for 2 h at 37 °C. Conversion of tetraubiquitin to free ubiquitin was monitored by SDS-PAGE followed by immunoblotting with anti-ubiquitin.

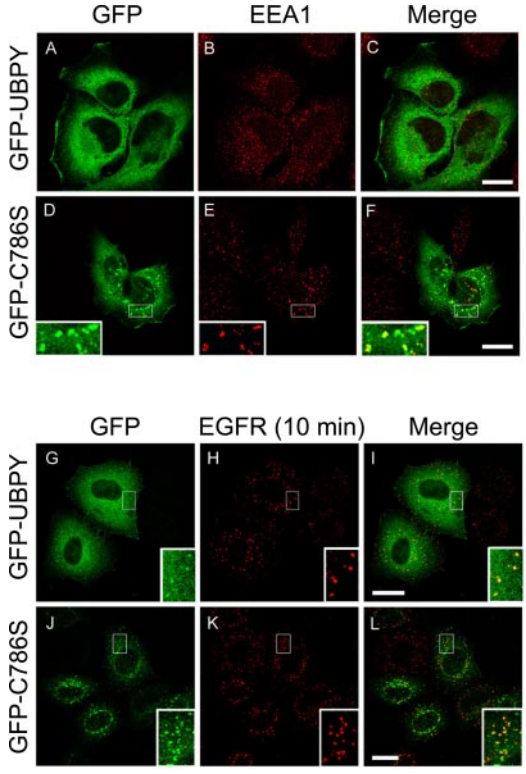

FIGURE 2. **Co-localization of UBPY with endosomal markers.** HeLa cells were transfected with GFP-UBPY (*A–C* and *G–I*) or with catalytically inactive GFP-UBPY(C786S) (*D–F* and *J–L*) and either stained with anti-EEA1 (shown in *red*, *A–F*) or first starved and then stimulated for 10 min with 100 ng/ml EGF before staining with anti-EGFR (shown in *red*, *G–L*). All panels represent confocal sections. *Insets* show 3-fold magnification of the boxed area. *Scale bar*, 20 μm.

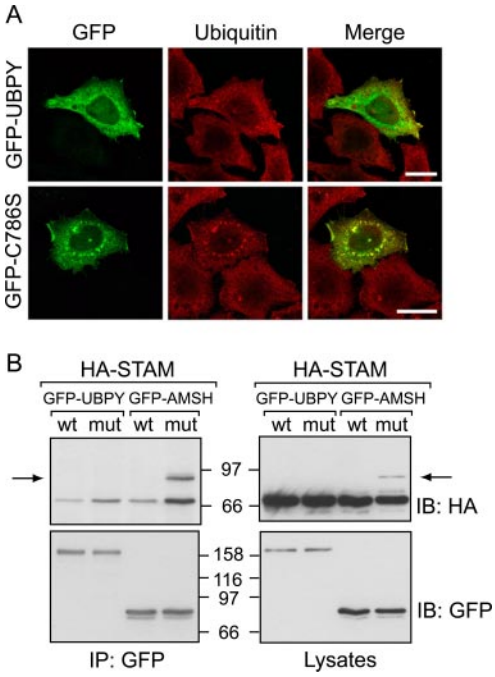

FIGURE 3. **Catalytically inactive UBPY promotes accumulation of ubiquitinated proteins on endosomes.** *A*, HeLa cells were transfected with GFP-UBPY or with catalytically inactive GFP-UBPY(C786S) and stained with anti-ubiquitin antibodies (shown in *red*). All panels represent confocal sections. *Scale bars*, 20 μm. *B*, HeLa cells were co-transfected with GFP-tagged wild-type (*wt*) UBPY or AMSH or catalytically inactive mutant (*mut*) UBPY(C786S) or AMSH(D348A) together with HA-STAM. Cells were lysed and GFP-tagged proteins immunoprecipitated (*IP*) and analyzed in parallel with the lysates (right-hand panels) by immunoblotting (*IB*) with anti-HA antibodies followed by reprobing with anti-GFP.

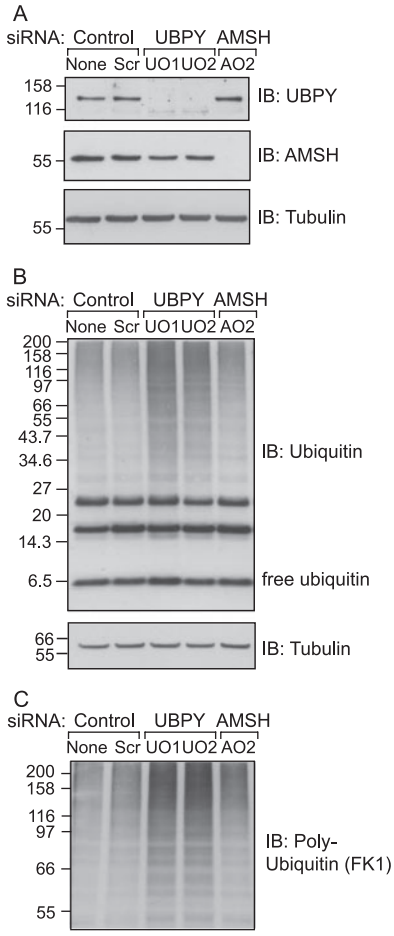

FIGURE 4. **Depletion of UBPY by siRNA promotes accumulation of polyubiquitinated proteins.** HeLa cells were treated with control siRNA (*Scr*), UBPY-specific siRNA oligonucleotides (*UO1*, *UO2*), or AMSH-specific siRNA (*AO2*) or left untreated (*None*). Cells were lysed after 96 h, and samples analyzed with anti-UBPY, anti-AMSH, and anti-tubulin antibodies (*A*), or with anti-ubiquitin antibodies that either recognize all species of ubiquitinated proteins including free ubiquitin (*B*) or specifically react with polyubiquitinated proteins (*C*, *FK1*). *IB*, immunoblot.

Electron Microscopy—Control and UBPY-depleted HeLa cells were incubated in media containing 10 mg/ml horseradish peroxidase (Sigma) for 30 min before fixing with 2% glutaraldehyde, 2% paraformaldehyde in phosphate buffer, pH7.4. Following cross-linking of horseradish peroxidase with 0.075% of 3,3′diaminobenzidine tetra hydrochloride (Sigma), 0.023% H_2O_2, cells were post-fixed with 2.5% glutaraldehyde, osmicated, stained en bloc with uranyl acetate and processed for Epon embedding according to standard procedures. Ultrathin (70 nm) sections were cut and stained with lead citrate before viewing in a Tecnai Spirit electron microscope. MVBs were identified morphologically by the presence of internal vesicles, and their maximal chord lengths were determined using AnalySIS (SIS, GmbH). Gross changes in MVB abundance were measured by counting MVBs in cells with a coincident nuclear profile and normalizing to the total cell area measured with AnalySIS (scrambled: cellular profiles counted $n = 22$, total area of cells examined = 3353 μm^2, MVBs counted $n = 156$; UBPY: cellular profiles counted $n = 23$, total area of cells examined area = 3382 μm^2, MVBs counted $n = 230$).

RESULTS

Substrate Specificity of UBPY—We have adapted an *in vitro* assay for DUB activity that monitors the processing of polyubiquitin chains to lower denomination forms (22, 30). In our original analysis, AMSH showed specificity for Lys-63-linked, whereas UBPY showed specificity for Lys-48-linked polyubiquitin (22). This observation came with the caveat that the Lys-63-linked chains available to us at that time were derived from mutant ubiquitin in which all lysines, with the exception of Lys-63, had been converted to arginines. We have now repeated these experiments with polyubiquitin chains derived from wild-type ubiquitin and find that in contrast to AMSH, UBPY shows little discrimination between Lys-48 and Lys-63-linked chains (Fig. 1).

Subcellular Distribution of UBPY—We next analyzed the subcellular localization of UBPY and a catalytically inactive mutant UBPY (C786S) (23) in HeLa cells. We analyzed cells expressing low levels of GFP-tagged UBPY and UBPY (C786S) because our UBPY antibody is not sensitive enough to pick up the endogenous protein. In untreated cells, both wild-type and inactive UBPY are localized to the cytosol and plasma membrane (Fig. 2). UBPY (C786S) shows an additional staining of punctate structures, identified as early endosomes by co-localization with anti-EEA1 (Fig. 2, *D–F*) and with internalized EGFR (*J–L*). Interestingly, wild-type UBPY appears to be recruited to EGFR-containing early endosomes upon stimulation (Fig. 2, *G–I*).

Regulation of Ubiquitin Dynamics—Expression of catalytically inactive, but not wild-type, UBPY causes a build up of ubiquitin on endosomes; a phenomenon we have previously observed following expression of catalytically inactive AMSH (D348A) (Fig. 3*A*) (22). However, in contrast to AMSH (D348A), this UBPY (C786S) mutant does not promote accumulation of a higher molecular mass (+14 kDa) form of STAM (Fig. 3*B*), which is recognized by ubiquitin antibodies (22).

Both UBPY and AMSH associate with the SH3 domain of STAM via the same type of non-canonical P*XX*P motif and hence may compete for binding (19). Effects due to overexpression of catalytically inactive mutants could reflect displacement of either endogenous UBPY or AMSH. We therefore turned to RNA interference to address the role of

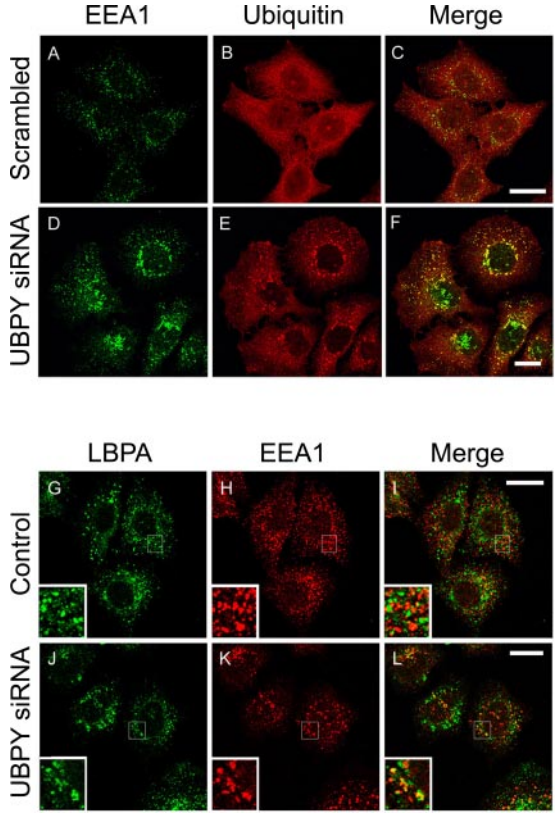

FIGURE 5. **Depletion of UBPY by siRNA promotes accumulation of ubiquitin on aberrantly enlarged endosomes.** HeLa cells were treated with control siRNA (*Scrambled*, *A–C*), UBPY-specific siRNA (*D–F* and *J–L*) or mock-treated (*G–I*). Cells were fixed, permeablized, and co-stained for ubiquitin (shown in *red*, *A–I*) and EEA1 (in *green*) or LBPA (in green, *G–L*) and EEA1 (in *red*). All panels represent confocal sections. *Insets* show 3-fold magnification of the boxed area. *Scale bars*, 20 μm.

UBPY in endosomal ubiquitin dynamics (Fig. 4*A*). Neither treatment of cells with transfection reagent alone, control (scrambled) siRNA, nor specific AMSH siRNA had any effect on the overall levels of ubiquitinated proteins as detected by Western blotting (Fig. 4*B*). In contrast, knockdown of UBPY, achieved independently with two distinct siRNA oligonucleotides, resulted in a clear increase in the level of ubiquitinated proteins. Many of these proteins are polyubiquitinated, based on Western blotting with a polyubiquitin specific antibody (FK1 (4)) (Fig. 4*C*). Although overall ubiquitination was increased, no depletion in the levels of free ubiquitin was observed in UBPY knockdown cells (Fig. 4*B*). Immunofluorescence microscopy on UBPY knockdown cells revealed an accumulation of ubiquitin on endosomes in 84.7 ± 4.5% ($n = 5$, total number of cells counted 1474) of the cells treated with UBPY Oligo1 and 83.2 ± 3.2% ($n = 4$, total number of cells counted 977) treated with Oligo2, which was not observed in control cells (0.3 ± 0%, $n = 3$, total number of cells counted 1006) (Fig. 5, *A–F*). These could be co-labeled with EEA1, which exhibits a corresponding redistribution to ubiquitin-positive perinuclear clusters in addition to more characteristic peripheral punctae.

Morphological Changes—Using confocal immunofluorescence microscopy, we noticed an increased apposition between EEA1-positive endosomes and structures containing LBPA, a late endosomal/lysosomal marker (Fig. 5, *G–L*) (2, 31). Examination of UBPY knockdown cells by transmission electron microscopy revealed that knockdown cells contained an increased number of multivesicular endosomal profiles (45% increase of MVBs/μm^2, $p < 0.038$), which also showed a significant difference in size distribution with 30.4% of MVBs in UBPY-depleted cells having a maximum diameter of >800 nm as compared with 9.4% in control-treated cells

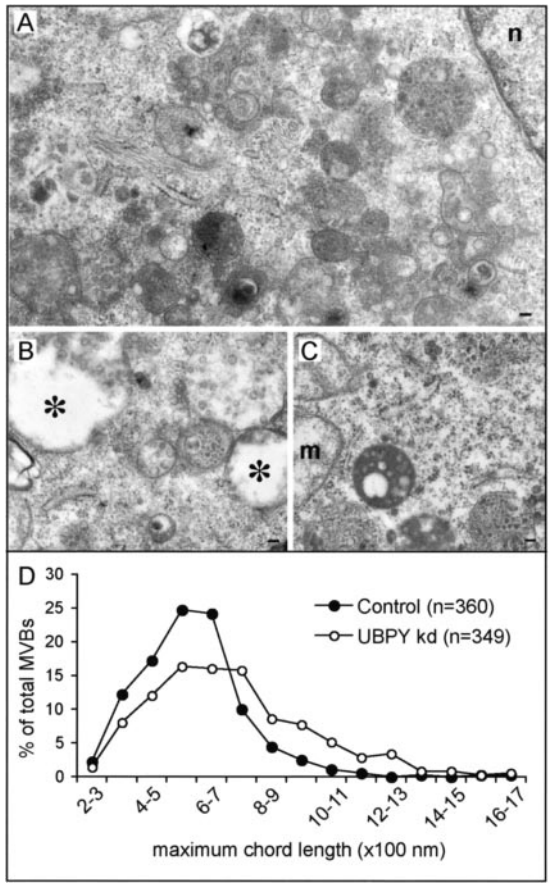

FIGURE 6. **UBPY knockdown promotes accumulation of aberrant pleomorphic multivesicular structures.** Tightly aggregated MVBs that accumulate in the perinuclear area are a hallmark of HeLa cells treated with UBPY-specific siRNA oligonucleotides (*A*). Aberrant MVBs of large diameter some containing only few internal vesicles (*) can also be observed in UBPY- (*B*) but not control siRNA-treated cells (*C*). Analysis of size distributions based on maximal chord lengths reveals a pool of enlarged MVBs in UBPY knockdown cells (*D*). MVBs are also 45% more abundant in UBPY-depleted cells ($p < 0.038$). *n* = nucleus; *m* = mitochondrion; *bars* = 100 nm.

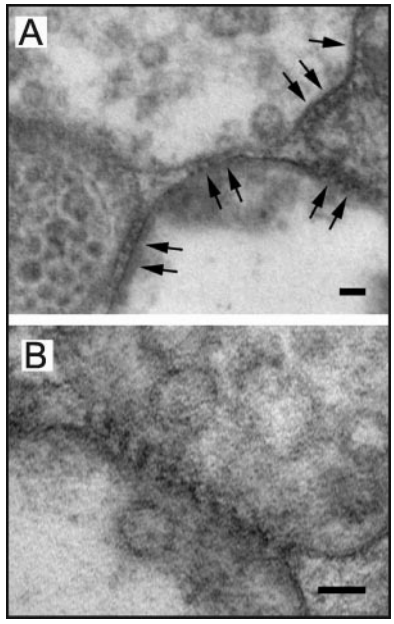

FIGURE 7. **UBPY knockdown promotes accumulation of MVBs that are attached to each other via distinctive tethers.** Clusters of endosomes display an unusual regular tethering arrangement (*arrows*, *A* and *B*) that is not seen in control cells. *Bars* = 50 nm.

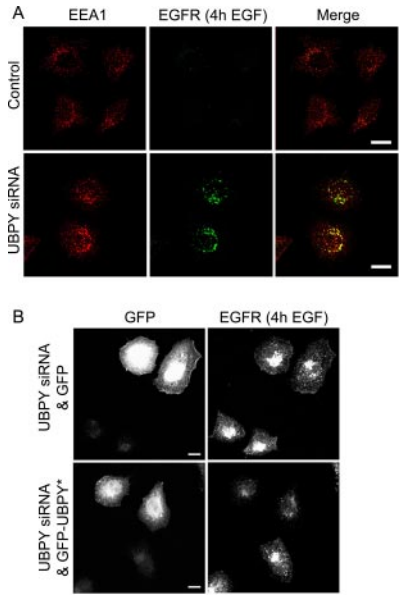

FIGURE 8. **Depletion of UBPY by siRNA inhibits EGF-dependent EGFR down-regulation.** *A*, HeLa cells were treated either with control siRNA (scrambled) or UBPY-specific siRNA, starved, and then stimulated with 100 ng/ml EGF for 4 h before staining with anti-EGFR. *Scale bar*: 20 μm. *B*, HeLa cells were treated with UBPY-specific siRNA and subsequently transfected either with GFP alone or siRNA-resistant UBPY (UBPY*). Cells were starved and stimulated as in *A* before staining with anti-EGFR. Cells expressing GFP-UBPY* but not GFP alone show reduced levels of undegraded EGFR, suggesting that the degradation of activated EGFR has been restored by recomplementation of UBPY. *Scale bar*: 10 μm. All panels represent confocal sections.

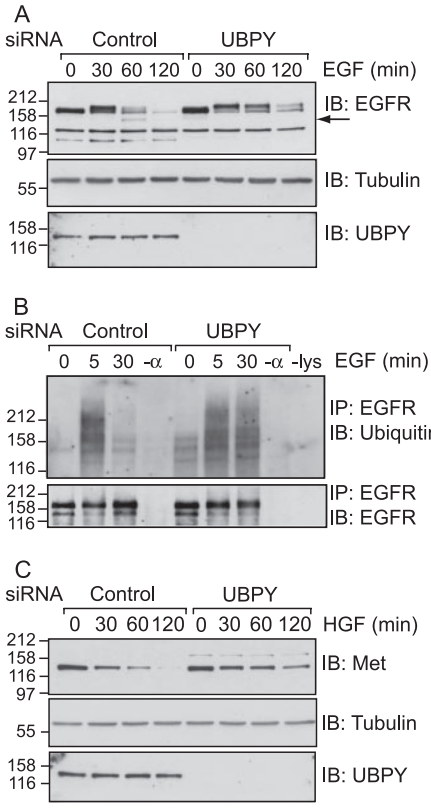

FIGURE 9. **UBPY is required for the down-regulation of acutely stimulated receptor tyrosine kinases.** *A* and *C*, HeLa cells were treated either with control siRNA or UBPY-specific siRNA, starved, and stimulated with 100 ng/ml EGF or 250 ng/ml HGF for indicated times. Cells were then lysed, and protein samples were analyzed by immunoblotting (*IB*) with anti-UBPY and anti-EGFR and anti-Met antibodies. Equal loading was assessed by reprobing with anti-tubulin. Note the appearance of a diagnostic EGFR degradation product (*arrow* in *A*) at 60 min in control cells that is absent from UBPY knockdown cells. *B*, HeLa cells were treated as in *A*, lysed, and immunoprecipitated with anti-EGFR or without antibody (-α). As a further control, a mock-immunoprecipitation without lysate was carried out in parallel (*-lys*). Immunoprecipitates were analyzed by immunoblotting with anti-ubiquitin (*top*) and anti-EGFR (*bottom*).

(Fig. 6, *A* and *D*). Another striking feature is the induction of vacuolar structures, which appear largely empty save for a few luminal vesicles and which are not seen in control cells (Fig. 6, compare *B* with *C*). Electron microscopy also provides striking views of large numbers of MVBs "stitched together" along extended areas of close contact by a regularly spaced repeating unit of electron-dense material with a characteristic length of 23.3 $\pm$ 3.1 nm (n = 33) (Fig. 7).

Regulation of RTK Dynamics—EEA1 containing endosomes in UBPY-depleted cells were accessible to internalized EGFR (and EGF) but in distinction to endosomes in control cells, retained the receptor for extended time periods and protected it from degradation (Fig. 8*A*). This delay in EGFR degradation could be directly attributed to the loss of UBPY, because overexpression of siRNA-resistant GFP-tagged UBPY (UBPY*), but not GFP alone, was able to rescue this phenotype (Fig. 8*B*). Co-expression of GFP-UBPY* during the last 66 h of the siRNA-mediated UBPY knockdown, significantly attenuated the delay in EGFR degradation: only 9.8% of GFP-UBPY*-transfected cells showed endosomal EGFR retention after 4 h of EGF treatment, compared with 75.4% of cells transfected with GFP alone. Likewise, only 3.1% of GFP-UBPY*-expressing cells showed an aberrant accumulation of ubiquitin on endosomes as compared with 77% of GFP-expressing cells (not shown). We further confirmed that EGFR down-regulation was defective in UBPY knockdown cells, by analyzing the same type of experiment using Western blotting of cell lysates (Fig. 9*A*). Following 60 min of acute EGF stimulation, we routinely detect a diagnostic EGFR degradation product that accompanies loss of full-length receptor (indicated by an *arrow*). This fragment is not generated in UBPY knockdown cells, and the lifetime of the receptor is significantly extended. It should however be noted that although this is a very clear block, a slow decline in EGFR levels is evident nevertheless. We next monitored the ubiquitination status of the EGFR upon EGF stimulation and found that deubiquitination of EGFR is severely impaired in UBPY-depleted cells (Fig. 9*B*), suggesting that UBPY activity may be required for removal of ubiquitin from EGFR prior to incorporation into MVBs.

We wondered whether the requirement of UBPY activity was specific to the down-regulation of EGFR or whether our observation would translate to other RTKs. We therefore analyzed the down-regulation of Met, the receptor for hepatocyte growth factor/Scatter factor in UBPY knockdown cells. Met receptor degradation requires both ubiquitination and endocytosis (6, 32), although, in distinction to EGFR, it also shows sensitivity to proteasome inhibitors through an indirect effect on its trafficking itinerary (33). Met receptor degradation is highly sensitive to UBPY knockdown and, as for EGFR, the degradation rate is significantly slowed in the absence of UBPY (Fig. 9*C*).

UBPY Regulates the Stability of the Hrs-STAM Complex—How can knockdown of a DUB retard RTK trafficking while free ubiquitin levels remain unaltered? One possibility is that UBPY can somehow regulate the MVB sorting machinery rather than act on the receptors themselves. We analyzed the distribution of Hrs in cells that were either mock-treated or depleted of UBPY or AMSH. In control, as well as in AMSH-depleted cells, Hrs is distributed between a major cytosolic and an endosomal pool, which presents as a mixture of peripheral punctate structures and a more tubulo-reticular perinuclear staining. This distribution is dramatically changed in UBPY-depleted cells; the cytosolic pool is largely depleted, and Hrs is recruited to aberrantly large perinuclear structures (Fig. 10*A*), which also label for ubiquitin (Fig. 5, *D–F*).

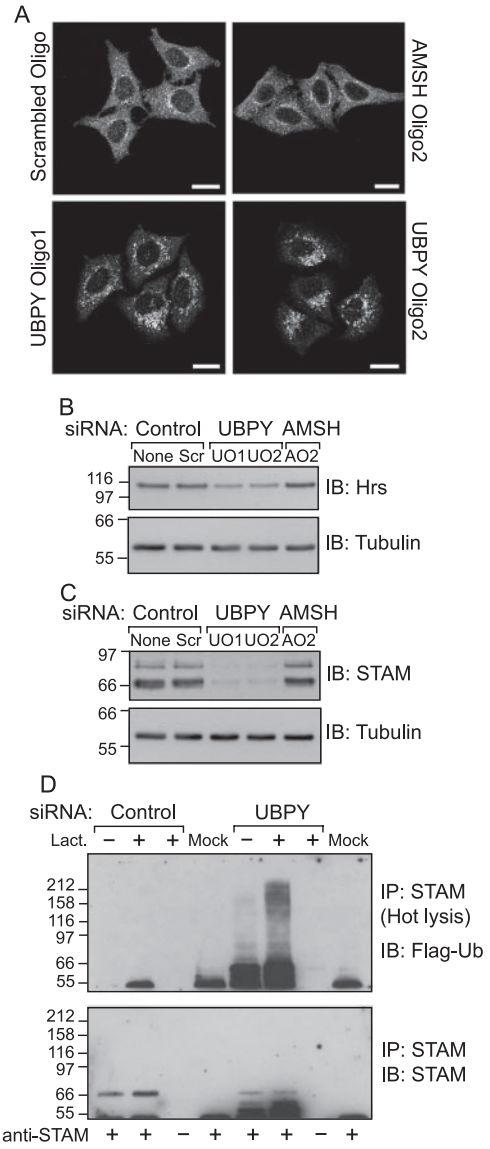

FIGURE 10. **siRNA knockdown of UBPY causes a redistribution of Hrs and severe depletion of STAM protein levels.** HeLa cells treated as in Fig. 4 were fixed and stained with anti-Hrs (*A*) or lysed in hot SDS-lysis buffer and probed with antibodies against Hrs and STAM (*B* and *C*). Equal loading was assessed by reprobing with anti-tubulin. *D*, HeLa cells were treated with control siRNA or UBPY-specific siRNA, transfected with FLAG-tagged ubiquitin (*Ub*), and incubated with lactacystin (*Lact.*) or Me_2SO for 7 h. Lysates were prepared as in *B* and *C* and STAM was immunoprecipitated and probed with horseradish peroxidase-coupled anti-FLAG followed by reprobing with anti-STAM. *IB*, immunoblot.

We further analyzed SDS-lysates of these cells by Western blotting and found that the total levels of Hrs were significantly decreased (50.2 ± 6.0%, $n = 3$) (Fig. 10*B*). Even more dramatically, we found that the Hrs-associated adapter protein STAM was effectively depleted in UBPY knockdown cells (Fig. 10*C*, >90% depleted, $n = 3$). However, over-expression of STAM in UBPY knockdown cells cannot rescue the observed defect in EGFR degradation (not shown). DUBs may stabilize proteins by opposing their ubiquitin-dependent proteasomal degradation. To test whether this might be the case for regulation of STAM levels, we treated UBPY knockdown Flag-Ubiquitin-transfected cells with the proteasomal inhibitor lactacystin. Following lysis of cells under denaturing conditions with SDS-containing buffer (hot SDS-lysis), STAM was immunoprecipitated and probed by Western blotting with anti-FLAG antibodies. Our data indicate that proteasomal inhibition in UBPY knockdown cells accumulates ubiquitinated STAM, which runs as a higher molecular weight smear (Fig. 10*D*). The presence of this ubiquitin smear is entirely contingent on the knockdown of UBPY. Interestingly, the levels of AMSH also appeared consistently lower in cells depleted of UBPY, (Fig. 4*A*; Oligo1 51.03% ± 9.67, $n = 3$; Oligo2 70.93% $n = 2$, percent of AMSH levels in control cells). It should be noted that this concomitant loss of AMSH cannot account for the observed phenotype because depletion of AMSH enhances rather than delays EGFR down-regulation (22) and does not cause the dramatic morphological changes we are reporting here.

DISCUSSION

UBPY is a DUB enzyme that shows no substantial discrimination between Lys-48- and Lys-63-linked polyubiquitin and may also act upon monoubiquitinated substrates, such as the platelet-derived growth factor receptor and EGFR (Fig. 1 and Ref. 34). At least one of the six other internal lysines within ubiquitin is required for its activity against Lys-63-linked polyubiquitin, as no activity is detected when these are mutated (22). Its depletion leads to a global accumulation of ubiquitinated proteins (Fig. 4 (23)) without depleting free ubiquitin levels.

We were interested in comparing the cellular properties of UBPY with AMSH. These two DUBs share a common binding site with the SH3 domain of STAM (19) but belong to different DUB families, USP/UBP and JAMM/MPN+, respectively. In contrast to AMSH, UBPY shows no association with endosomes in starved cells but can be recruited following acute EGF stimulation. A recent paper (34) suggests that UBPY directly interacts with EGFR, although we observed EGF-dependent translocation to endosomes at earlier time points (*e.g.* 10 min) than reported for this interaction (between 60 and 120 min). Catalytically inactive UBPY is found on endosomes in untreated cells, suggesting that its catalytic cycle may be necessary for dissociation from membranes. Catalytically inactive AMSH also shows more pronounced endosomal staining, and its overexpression, like that of UBPY, leads to pronounced accumulation of ubiquitin at endosomes. Both effects could be because of the displacement of endogenous AMSH or UBPY from their shared binding site to STAM.

We found that catalytically inactive AMSH but not UBPY promotes the appearance of a ubiquitinated form of STAM, with which it preferentially associates. For reasons still not fully appreciated, several DUBs physically interact with E3 ligases. Intriguingly, AMSH has been shown to interact with the RING-finger protein RNF11, which acts as an adapter for recruitment of the HECT E3-ligases Smurf1/2 and AIP4/Itch (35). Although ubiquitination of STAM is not well characterized, one report has implicated AIP4 in the ubiquitination of its binding partner Hrs (36). It may be that AMSH specifically recruits an E3 ligase to ubiquitinate STAM, which is exclusively stabilized by the catalytically inactive form of AMSH.

Knockdowns of AMSH and UBPY reveal stark differences. Only UBPY knockdown leads to changes in the distribution and size of endosomes as judged by immunofluorescence microscopy and to the accumulation of both Hrs and ubiquitin at their surface. This led us to examine the morphology of endosomal compartments in UBPY knockdown cells using transmission electron microscopy. There is clearly no block to luminal vesicle formation in these cells, as MVBs were in fact more abundant. Clusters of MVBs are apparently "stitched" together by a repeating electron dense structure. We speculate that this could correspond to ubiquitinated proteins recognized in *trans* by ubiquitin binding motifs on the partner endosomes. Thus, one aspect of UBPY function may be to disassemble these tethering structures.

Our biochemical and light microscopic analyses indicate that knock-

down of UBPY inhibits RTK degradation. Intriguingly this contrasts with the AMSH knockdown phenotype for which the rate of EGFR degradation is clearly enhanced (22). Mizuno *et al.* (34) have recently reported a moderate enhancement of EGFR receptor down-regulation kinetics in UBPY knockdown cells, which is in direct opposition to the data presented here. Our experiments have been repeated using independent transient transfection of two UBPY-specific siRNA duplexes, whereas the previous findings by Mizuno *et al.* (34) were based on transient expression of a single short hairpin pSILENCER construct. In addition we have been able to rescue the loss of EGFR-degradation by overexpressing siRNA-resistant GFP-UBPY. While our manuscript was under revision, an unrelated report by Bowers *et al.* (37) compared the effect of UBPY and AMSH depletion on ^{125}I-labeled EGF degradation and is in agreement with our findings.

UBPY is proposed to be an orthologue of the yeast enzyme Doa4, the deletion of which leads to impaired receptor sorting (26). Doa4 function is not thought to be essential for the sorting step, but rather acts to maintain the necessary cellular levels of free ubiquitin. We observed no depletion in the levels of ubiquitin following UBPY knockdown suggesting that this is not the mechanism by which receptor sorting is disrupted. How then can the loss of a DUB lead to an inhibition of receptor down-regulation? One possibility is that UBPY knockdown leads to the accumulation of aberrantly ubiquitinated receptors, which can no longer be degraded. An alternative explanation may lie in the significant depletion of key proteins implicated in MVB sorting that associate with UBPY. Hrs levels are reduced by ~50%. On its own this is unlikely to lead to a pronounced defect in RTK sorting as higher levels of Hrs depletion lead to a much more modest suppression of Met degradation than we see here (2, 7). However, in UBPY-knockdown cells, this is accompanied by an almost complete loss of the Hrs-associated protein and UBPY binding partner, STAM. Our data suggest that UBPY may regulate STAM stability by reversing its polyubiquitination, which in the absence of UBPY targets STAM for proteasomal degradation. This may well contribute to the observed sorting defect because Kanazawa *et al.* (38) have previously shown that STAM −/− mouse embryonic fibroblasts are defective in EGFR degradation, and deletion of the yeast orthologue Hse1 also leads to defects in receptor sorting (39). However, it is most likely that the pleomorphic effects we observe at the ultrastructural level, as well as the global accumulation of polyubiquitinated proteins in UBPY knockdown cells, testify to the existence of multiple targets for UBPY activity.

In conclusion, the endosomal functions of the two STAM-interacting DUBs, UBPY and AMSH, are not redundant, with contrasting effects on the stability and ubiquitination status of STAM itself to the fore. UBPY may have multiple effects on endosomal compartments, which manifest as decreased rates of receptor down-regulation and accentuated tethering structures.

Acknowledgments—We thank Giulio Draetta, Francis Barr, Naomi Kitamura, John O'Bryan, and Jean Gruenberg for generously providing reagents.

REFERENCES

1. Felder, S., Miller, K., Moehren, G., Ullrich, A., Schlessinger, J., and Hopkins, C. R. (1990) *Cell* **61,** 623–634
2. White, I. J., Bailey, L. M., Aghakhani, M. R., Moss, S. E., and Futter, C. E. (2005) *EMBO J.* **25,** 1–12
3. Katzmann, D. J., Sarkar, S., Chu, T., Audhya, A., and Emr, S. D. (2004) *Mol. Biol. Cell* **15,** 468–480
4. Haglund, K., Sigismund, S., Polo, S., Szymkiewicz, I., Di Fiore, P. P., and Dikic, I. (2003) *Nat. Cell Biol.* **5,** 461–466
5. Mosesson, Y., Shtiegman, K., Katz, M., Zwang, Y., Vereb, G., Szollosi, J., and Yarden, Y. (2003) *J. Biol. Chem.* **278,** 21323–21326
6. Peschard, P., Fournier, T. M., Lamorte, L., Naujokas, M. A., Band, H., Langdon, W. Y., and Park, M. (2001) *Mol. Cell* **8,** 995–1004
7. Hammond, D. E., Carter, S., McCullough, J., Urbé, S., Vande Woude, G., and Clague, M. J. (2003) *Mol. Biol. Cell* **14,** 1346–1354
8. Urbé, S., Sachse, M., Row, P. E., Preisinger, C., Barr, F. A., Strous, G., Klumperman, J., and Clague, M. J. (2003) *J. Cell Sci.* **116,** 4169–4179
9. Raiborg, C., Bache, K. G., Gillooly, D. J., Madshus, I. H., Stang, E., and Stenmark, H. (2002) *Nat. Cell Biol.* **4,** 394–398
10. Hicke, L., and Dunn, R. (2003) *Annu. Rev. Cell Dev. Biol.* **19,** 141–172
11. Ciechanover, A. (2005) *Nat. Rev. Mol. Cell. Biol.* **6,** 79–86
12. Deveraux, Q., Ustrell, V., Pickart, C., and Rechsteiner, M. (1994) *J. Biol. Chem.* **269,** 7059–7061
13. Chau, V., Tobias, J. W., Bachmair, A., Marriott, D., Ecker, D. J., Gonda, D. K., and Varshavsky, A. (1989) *Science* **243,** 1576–1583
14. Pickart, C. M., and Fushman, D. (2004) *Curr. Opin. Chem. Biol.* **8,** 610–616
15. Dupre, S., Urban-Grimal, D., and Haguenauer-Tsapis, R. (2004) *Biochim. Biophys. Acta* **1695,** 89–111
16. Nijman, S. M., Luna-Vargas, M. P., Velds, A., Brummelkamp, T. R., Dirac, A. M., Sixma, T. K., and Bernards, R. (2005) *Cell* **123,** 773–786
17. Amerik, A. Y., and Hochstrasser, M. (2004) *Biochim. Biophys. Acta* **1695,** 189–207
18. Tanaka, N., Kaneko, K., Asao, H., Kasai, H., Endo, Y., Fujita, T., Takeshita, T., and Sugamura, K. (1999) *J. Biol. Chem.* **274,** 19129–19135
19. Kato, M., Miyazawa, K., and Kitamura, N. (2000) *J. Biol. Chem.* **275,** 37481–37487
20. Maytal-Kivity, V., Reis, N., Hofmann, K., and Glickman, M. H. (2002) *BMC Biochem.* **3,** 28
21. Cope, G. A., Suh, G. S., Aravind, L., Schwarz, S. E., Zipursky, S. L., Koonin, E. V., and Deshaies, R. J. (2002) *Science* **298,** 608–611
22. McCullough, J., Clague, M. J., and Urbé, S. (2004) *J. Cell Biol.* **166,** 487–492
23. Naviglio, S., Mattecucci, C., Matoskova, B., Nagase, T., Nomura, N., Di Fiore, P. P., and Draetta, G. F. (1998) *EMBO J.* **17,** 3241–3250
24. Bowers, K., Lottridge, J., Helliwell, S. B., Goldthwaite, L. M., Luzio, J. P., and Stevens, T. H. (2004) *Traffic* **5,** 194–210
25. Luhtala, N., and Odorizzi, G. (2004) *J. Cell Biol.* **166,** 717–729
26. Amerik, A. Y., Nowak, J., Swaminathan, S., and Hochstrasser, M. (2000) *Mol. Biol. Cell* **11,** 3365–3380
27. Dupre, S., and Haguenauer-Tsapis, R. (2001) *Mol. Cell. Biol.* **21,** 4482–4494
28. Sachse, M., Urbé, S., Oorschot, V., Strous, G. J., and Klumperman, J. (2002) *Mol. Biol. Cell* **13,** 1313–1328
29. Row, P. E., Clague, M. J., and Urbé, S. (2005) *Biochem. J.* **389,** 629–636
30. Hartmann-Petersen, R., Hendil, K. B., and Gordon, C. (2003) *FEBS Lett.* **535,** 77–81
31. Kobyashi, T., Stang, E., Fang, K. S., de Moerloose, P., Parton, R. G., and Gruenberg, J. (1998) *Nature* **392,** 193–197
32. Hammond, D. E., Urbé, S., Vande Woude, G. F., and Clague, M. J. (2001) *Oncogene* **20,** 2761–2770
33. Carter, S., Urbé, S., and Clague, M. J. (2004) *J. Biol. Chem.* **279,** 52835–52839
34. Mizuno, E., Iura, T., Mukai, A., Yoshimori, T., Kitamura, N., and Komada, M. (2005) *Mol. Biol. Cell* **16,** 5163–5174
35. Li, H., and Seth, A. (2004) *Oncogene* **23,** 1801–1808
36. Marchese, A., Raiborg, C., Santini, F., Keen, J. H., Stenmark, H., and Benovic, J. L. (2003) *Dev. Cell* **5,** 709–722
37. Bowers, K., Piper, S. C., Edeling, M. A., Gray, S. R., Owen, D. J., Lehner, P. J., and Luzio, J. P. (2006) *J. Biol. Chem.* **281,** 5094–5105
38. Kanazawa, C., Morita, E., Yamada, M., Ishii, N., Miura, S., Asao, H., Yoshimori, T., and Sugamura, K. (2003) *Biochem. Biophys. Res. Commun.* **309,** 848–856
39. Bilodeau, P. S., Urbanowski, J. L., Winistorfer, S. C., and Piper, R. C. (2002) *Nat. Cell Biol.* **4,** 534–539